Scanning Probe Microscopy (SPM)

Difficulties in monitoring, characterizing and manipulation processes at extreme small dimensions(1 A) .

Experimental tools for imaging the local atomic topography; mechanical, electronic and transport properties of samples at dimensions ranging from the mesoscale to the nanoscale.

Understanding of the interaction between the probe and the sample (substrate).

Electronic and mechanical processes governing the image formation.

SPM works with a conducting tip held at a given electric potential. Weak interaction → tunneling

Strong interaction → mechanical properties

1- Scanning Tunneling Microscopy (STM)

Approach for image simulation based on Tersoff-Hamann approximation.

Electron flow from the tip to the sample is given by the convolution of the electronic densities of states of the tip and the sample within the potential bias window centered on the common Fermi level.

In approach, the coupling of the tip to the sample is treated as a perturbation of the sample/substrate Hamiltonian and first-order perturbation theory.

Only weak couplings (tunneling regime) can be treated in this manner, rules out contact modes, field-effects and strong interaction in general.

Based on the detection of AC or DC current induced by a bias applied to the sample and/or to the tip. The spatial resolution of these techniques is determined by the contact separation and the exact nature of the probe-sample interaction.

- Electronic Tunneling

Tunneling phenomena have been studied for long time is well understood in terms of quantum theory as shown in Fig. 1.

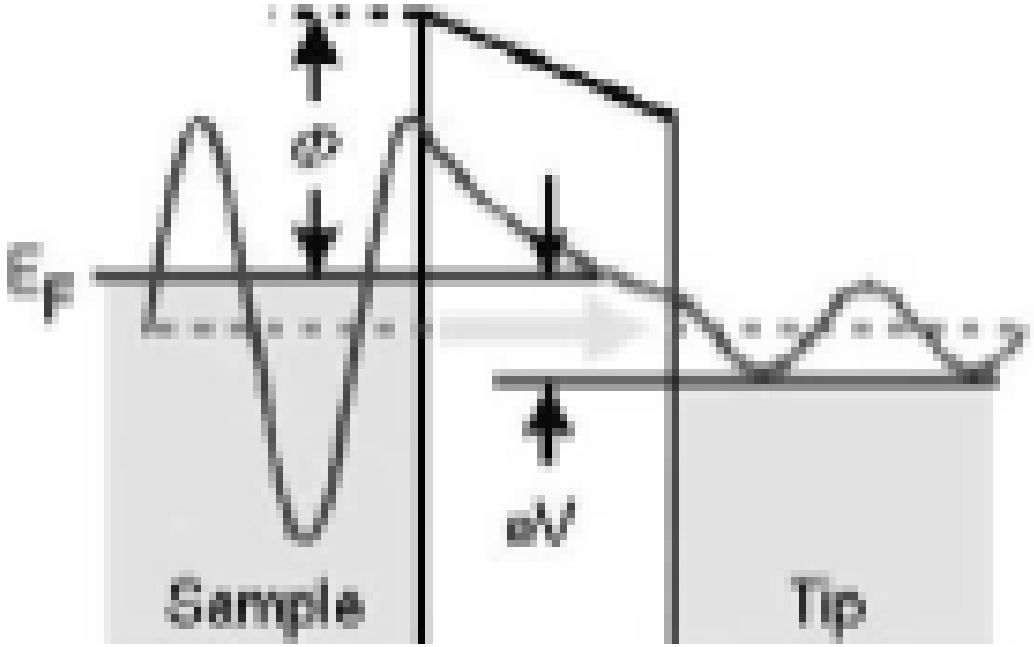

Figure 1 – A one dimensional barrier between two metal electrodes. A bias voltage of V is applied between the electrodes.

Considering an one-dimensional vacuum barrier between two electrodes (the sample and the tip) and assuming their work functions to be the same and the barrier height to be Φ, if a bias voltage of V is applied between the two electrodes with a barrier width d, according to quantum theory under first-order perturbation [J. Bardeen, Phys. Rev. Lett. **6**, 57 (1961)] the tunneling current is

$$I = \frac{2\pi e}{\hbar} \sum_{\mu,\nu} f(E_\mu)[1 - \int (E_\nu + eV)] \left| M_{\mu\nu} \right|^2 \delta(E_\mu - E_\nu) \qquad (1)$$

where *f* (*E*) is the Fermi function, $M_{\mu\upsilon}$ *is the tunneling matrix element between states* ψ_μ *and* ψ_υ *of the respective electrodes,* E_μ *and* E_υ *are the energies of* ψ_μ *and* ψ_υ *, respectively. Under assumptions of small voltage and low temperature, the above formula can be simplified to*

$$I = \frac{2\pi}{\hbar} e^2 V \sum_{\mu,\nu} \left| M_{\mu\nu} \right|^2 \delta(E_\nu - E_F)\delta(E_\mu - E_F) \qquad (2)$$

Bardeen showed that under certain assumptions, the tunneling matrix element can be expressed as

$$M_{\mu\nu} = \frac{\hbar^2}{2m}\int dS \cdot (\psi_\mu \vec{\nabla}\psi_\nu - \psi_\nu \vec{\nabla}\psi_\mu) \qquad (3)$$

where the integral is over all the surfaces surrounding the barrier region. To estimate the magnitude of $M_{\mu\upsilon}$, the wave function of the sample ψ_υ *can be expanded in the generalized plane-wave form*

$$\psi_\nu = \Omega_s^{-1/2}\sum_G a_G \exp[(k^2 + \left|\vec{k}_G\right|^2)^{1/2} z]\exp(i\vec{k}_G \cdot \vec{x}) \qquad (4)$$

where Ω_s is the volume of the sample, $k = h^{-1}(2m\phi)^{1/2}$ is the decay rate, ϕ is the work function, $k_G = k_{||} + G$, $k_{||}$ is the surface component of Bloch vector and G is the surface reciprocal vector.

To calculate the tunneling current, it is necessary to know the tip wave function. Unfortunately, the actual atomic structure of the tip is unknown and, moreover, it is very difficult to calculate the tip wave function due to its very low symmetry.

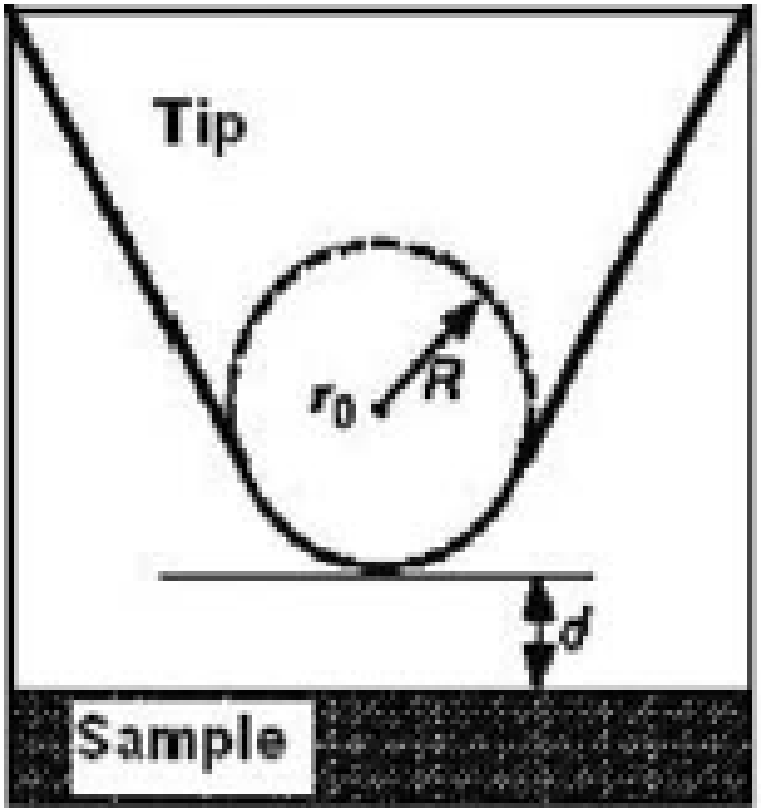

Figure 2- An ideal model for STM tip. The cusp of the tip is assumed to be a sphere with radius of R, the distance from the sample is d and the position of the center of the sphere is r_0.

- Operation

A weak potential difference is applied between the sample and a metallic tip.

The flow of a tunneling current is possible as long as the tip-sample distance is smaller than a few Angstroms.

The bias polarity, electron transfer can either be established from occupied states of the sample into unoccupied states of the tip (positive tip potential) or occupied states of the tip into unoccupied states of the sample (negative tip potential).

In topographic mode, a feedback mechanism permits tuning of the tip vertical position. STM image displays the variations of the tip vertical position while horizontally scanning the sample.

At constant height mode, maps of the tunneling current over the sample are obtained by varying the horizontal position of the tip. Applied bias up to about 1V, the tunneling rate is very sensitive to the electronic states close to the Fermi level.

The charge distribution of those states turns out to be a signature of the total charge. STM image reflects the atomic arrangements of the sample.

- Tersoff-Hamann approach essential

Physical system described a time-independent Hamiltonian H_0. Hamiltonian represents a system constituted by the sample and the STM tip. A linear combination of atomic orbital (LCAO) description, H_0 would be a matrix made up of two independent blocks H_0^s and H_0^t.

Suppose a time $t = 0$, the tip is brought in close contact (typically, a few Angstroms) with the sample, can be expressed as a perturbation $W(t) = \lambda\hat{W}(t)$ to the original system, where the matrix elements of $\hat{W}(t)$ are comparable in amplitude to those of H_0. Following time-dependent Hamiltonian

$$H(t) = H_0 + W(t) \qquad (1)$$

For $t < 0$, one assumes that the system is described by the state $|\varphi i\rangle$, which is an eigenstate of H_0. Transitions between the eigenstates of the system can be induced by turning on the perturbation $W(t)$. Quantitatively, the transitions can be computed as the probability $P_{if}(t)$ to find, at any time t, the system in an eigenstate $|\varphi_f\rangle$ of H_0, knowing that it was initially in the state $|\varphi_i\rangle$

$$P_{if}(t) = |\langle \varphi f \mid \psi(t) \rangle|^2 \qquad (2)$$

In the time interval between 0 and t, the state of the system obeys the time-dependent Schrodinger equation

$$i\hbar \frac{d}{dt}\left|\psi(t)\right\rangle = \left[H_0 + \lambda \hat{W}(t)\right]\left|\psi(t)\right\rangle \qquad (3)$$

with the following initial condition:

$$| \psi(t = 0) \rangle = | \varphi i \rangle \qquad (4)$$

In general, an analytic solution to Eq. (3) does not exist. However, if the perturbation W is weak (i.e., if λ is small), an approximate solution can be determined and P_{if} (t) can be calculated.

When a positive (negative) potential V is applied to the tip while the sample is set to the ground potential, all the tip states corresponding to E_v are lowered (raised) by –eV. At low temperature, tip states are occupied up to the Fermi level $E^t_F - eV$, which has also been shifted by eV (Fig. 3).

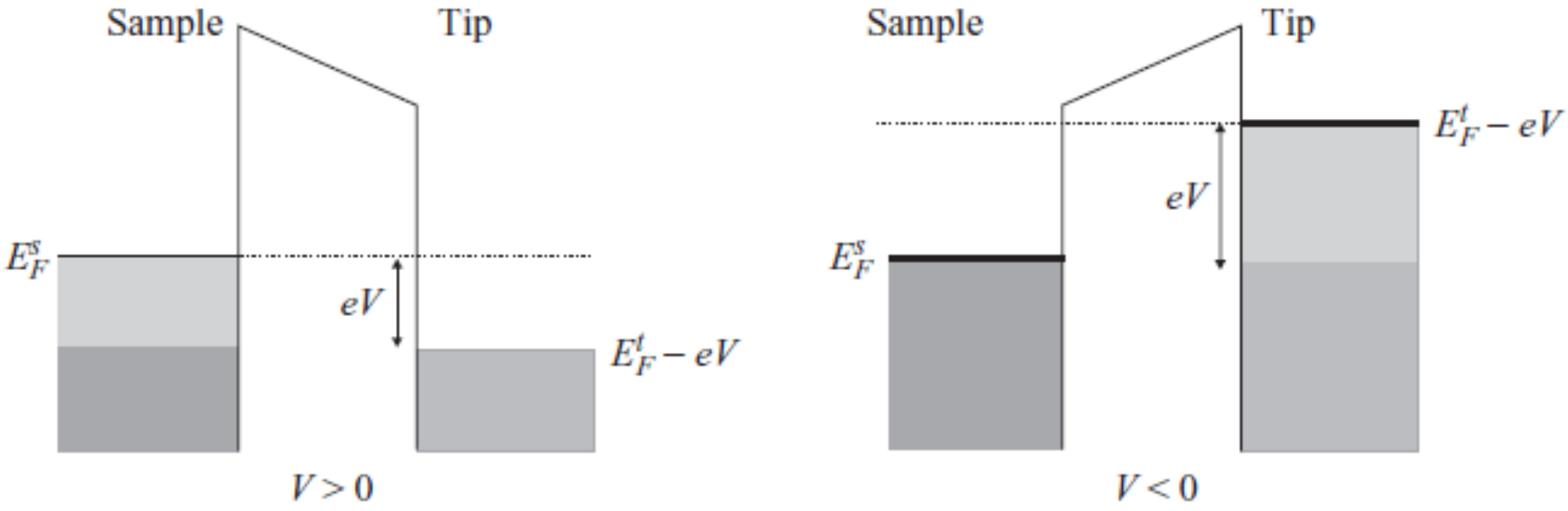

Figure 3- Schematic representation of the electronic processes governing the tunneling current in the presence of an external potential *V* between the tip and the sample. The electronic states at the Fermi level must overcome a potential barrier equal to the work function in order to tunnel. In the absence of the external potential, this barrier makes it impossible for the electrons to escape the sample or the tip. Note that the (un-)occupied states of the sample contribute to the tunneling current when the external tip potential is positive (negative).

However, for the tip we may adopt the reasonable model shown in Fig. 2, which was used by *Tersoff et al.* [J. Tersoff and D.R. Hamann, Phys. Rev. Lett, **31**, 805 (1985)] to describe an ideal tip and then the wave function of the tip is

$$\psi_\mu = \Omega_t^{-1/2} c_t k \,\mathrm{Re}^{kR} (k|\vec{r} - \vec{r}_o|)^{-1} e^{-k|\vec{r}-\vec{r}_o|} \qquad (5)$$

where Ω_t is the volume of the tip, c_t is a constant determined by the sharpness of the tip and its electronic structure. For simplicity, only the s-wave function of the tip is used in the calculation. Because of

$$(k\vec{r})^{-1} e^{-k\vec{r}} = \int d^2 q b(\vec{q}) \exp[-(k^2 + q^2)^{1/2} |z|] \exp(i\vec{q}\cdot\vec{x}) \qquad (6)$$

$$b(q) = (2\pi)^{-1} k^{-2} (1 + q^2/k^2)^{-1/2} \qquad (7)$$

substituting these wave functions to Eq. (3), we obtain

$$M_{\mu\nu} = \frac{\hbar^2}{2m} 4\pi k^{-1} \Omega_t^{-1/2} k \,\mathrm{Re}^{kR} \psi_\nu(\vec{r}_0) \qquad (8)$$

where r_0 is the position of the cusp center.

Substitute Eq. (8) to Eq. (2), we obtain

$$I = 32\pi^3 h^{-1} e^2 V \phi^2 D_t(E_F) R^2 k^{-4} e^{2kR} \sum_v \left|\psi_v(r_0)\right|^2 \delta(E_v - E_F) \qquad (9)$$

where $D_t(EF)$ is the density of states at the Fermi level for the tip.

Substituting the typical values for metals in Eq. (9), the tunneling current is obtained

$$I \propto V D_t(E_F) e^{2kR} \rho(r_0, E_F) \qquad (10)$$

$$\rho(r_0 E_F) = \sum \left|\psi_v(r_0)\right|^2 \delta(E_v - E_F) \qquad (11)$$

Thus, the STM with an s-wave tip would simply measure $\rho(r_0, E_F)$, which is the local density of states (DOS) at the Fermi level E_F and at a position r_0, the curvature center of the effective tip. Tersoff *et al.* also discussed the contribution of the tip wave function components of higher angular momentum, and found that these just made little difference for typical STM images. So, what the STM measures is only the property of the surface.

Because $|\psi_\upsilon(r_0)|^2 \propto e^{-2k(R+d)}$, thus $I \propto e^{-2kd}$. This means that the tunneling current depends on the tunneling gap distance d very sensitively. In the typical case, the tunneling current would change one order while the gap distance changes only 1 Å. This accounts for extremely high vertical resolution of 0.1 Å of STM.

Under these conditions, using the properties of the Fermi-Dirac distribution, in the low temperature limit, one finally obtains

$$I = \frac{2\pi e}{\hbar}\int_{-eV}^{0} dE \sum_{\mu\upsilon} \left|\left\langle \varphi_\mu \left| W \right| \varphi_\upsilon \right\rangle\right|^2 \delta\left(E - E_\mu + E_F^s\right)\delta\left(E - E_\upsilon + eV + E_F^t\right)$$

A STM probe is a nanoscale, often atomic scale and sharp *metallic* needle. When the tip is near the surface, usually in a few nanometer, with a voltage bias, tunneling currents flow between tip and surface. At a small bias voltage *V*, the tunneling current *I* can be approximated by

$$I \propto Ve^{-\frac{\sqrt{8m\phi}}{\hbar}d}$$

where *d* is the distance between STM tip and sample and ϕ is the work function of the tip.

2- Atomic Force Microscopy (AFM)

AFM can be operated in many modes and work on nonconducting materials

Image of many different types of materials such as:

- glass, polymers, metals, semiconductors
- nanomaterials
- biological samples.

AFM consists of a hard tip mounted on a cantilever.

The tip is brought in close proximity to the surface to be analyzed; the tip-sample interaction produces a deformation of the cantilever, which is measured

- Contact Mode

Tip very close to the surface, the force *F* exerted on it is dominated by the repulsive interaction between the tip apex and the nearest atoms of the surface, corresponding to the so-called contact mode.

- Non-contact Mode

AFM is also used in dynamical modes where the cantilever-tip assembly oscillating at a frequency close to its resonance. The sample is scanned while the feedback loop adjusts the tip-sample separation to keep the oscillation frequency (non-contact mode) or the amplitude of the oscillations (tapping mode) at a constant set-point value.

In the non-contact mode, the tip does not touch the sample.

In semi-contact or tapping mode, the oscillations bring the tip closer to the surface, in such a way that the tip partly probes the repulsive part of the interaction.

- First-principles theories applied to study the interaction between the AFM tip and the sample.

Interaction includes a repulsive part coming from the overlap of the core electron wave-functions

The decrease of the kinetic energy of the electrons due to their delocalization over tip and sample

The London dispersion interaction and of the other forces such as electrostatic and capillary forces.

The London dispersion force, simply called van der Waals interaction, may prevail over the first two contributions.

Density functional theory may fail in reproducing the dispersion force correctly.

Evaluating the force exerted on the tip in the repulsive regime is difficult, because both the sample and the tip are deformed and this problem is often addressed by molecular dynamics, most generally with empirical atomic potentials.

The simplest description of the tip-sample interaction relies on pair-wise potentials between the tip atoms (label *j*) and those (label *i*) of the sample,

$$V_{ts} = \sum_{i \in s} \sum_{j \in t} v_{ij}\left(r_{ij}\right) \qquad (1)$$

where V_{ij} can be, for instance, the Lennard-Jones 12-6 potential

$$V_{ij}(r_{ij}) = 4\varepsilon_{ij}\left[(\sigma_{if}/r_{ij})^{12} - (\sigma_{ij}/r_{ij})^{6}\right] \qquad (2)$$

The net force acting on the tip is readily deduced in the form

$$F_t = -\sum_{i \in s} \sum_{j \in t} \frac{dV_{ij}}{dr_{ij}} \frac{r_{ij}}{r_{ij}} \qquad (3)$$

The sums in the above expressions are replaced by integrals over simple shaped bodies.

The sample is represented by a half-space medium with a flat surface and if the tip is modeled by a paraboloid of revolution having its axis perpendicular to the surface, then

$$F_{tz} = \frac{B}{180}\frac{R_t}{z^8} - \frac{A}{6}\frac{R_t}{z^2} \qquad (4)$$

where R_t is the tip radius at the apex, z is the height of the tip apex above the sample surface, $B = 4\pi^2\varepsilon\sigma^{12}/\Omega_t\Omega_s$ and $A = B/\sigma^6$. Here, Ω_t and Ω_s are the atomic volumes of the tip and the sample, respectively. The second term is the London dispersion force.

Rather than integrating the r^{-6} part of the Lennard-Jones potential over the tip and sample, the London dispersion force can be evaluated by application of the Lifchitz theory, based on zero-point fluctuations of the electromagnetic field.

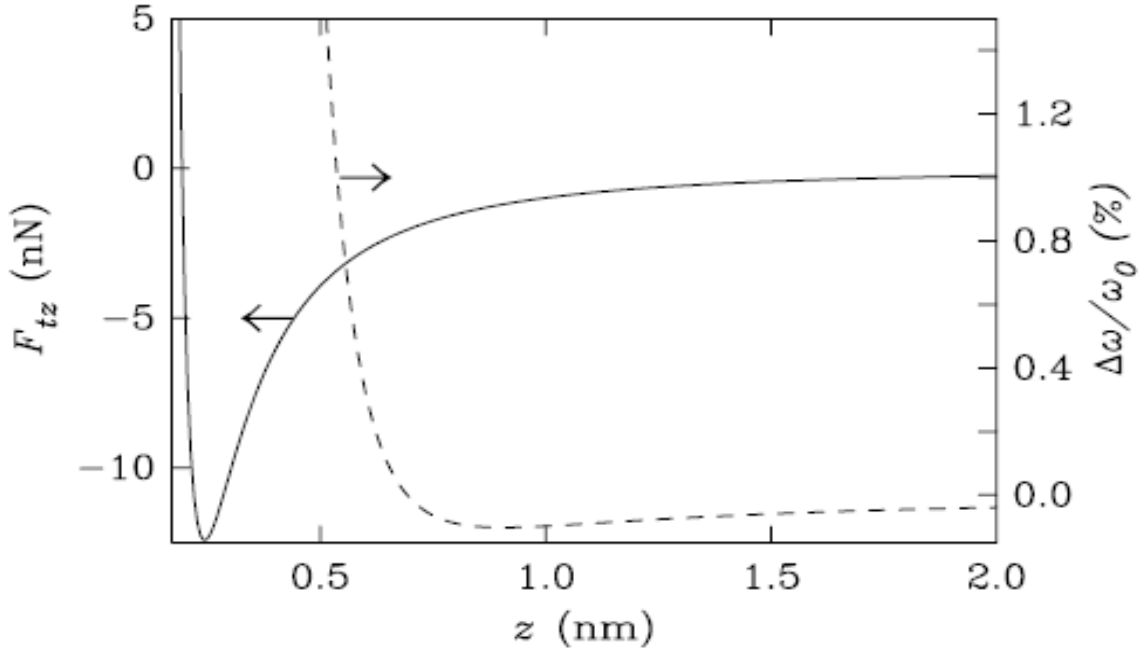

Figure 1- The vertical force exerted on an AFM diamond tip (Eq. (4), solid line) and the relative change of resonant frequency (Eq. (6), dashed line) versus the distance *z* of the tip apex above a graphite sample. The parameters used are ε = 2.97 meV, σ = 0.341 nm, *Rt* = 10 nm, *k* = 40N/m and *a* = 10 nm.

$$\Delta\omega/\omega_0 = \frac{1}{\sqrt{2}ka^{3/2}}\left(\frac{3003B}{512}\frac{R_1}{z^{15/12}} - \frac{A}{12}\frac{R_1}{z^{3/2}}\right) \qquad (6)$$

The implications of Eq. (4), though approximate, are twofold. First, the attractive part decreases slowly with increasing distance and it is rather long-ranged (Fig. 1). Second, the repulsive part of the tip-sample force is short-ranged. This part, however, is not well described by Eq. (4) at short distance. It is indeed important to take the atomic structure of the tip and sample into account when the distance between them is below one nanometer. In addition, the deformation of the sample and the tip softens their repulsive interaction.

In strong contact (indentation), most of the interaction is governed by the elastic, or even plastic, deformation of the two bodies. In the elastic domain, Hertz theory establishes that the force increases like the power 3/2 of the penetration $-\Delta z$ of the tip into the sample,

$$F_{tz} = (4/3)K_{ts}\sqrt{R_t}\,(-\Delta z)^{3/2} \qquad (5)$$

where $K_{ts} = [(1 - \nu_t^2)/Y_t + (1 - \nu_s^2)/Y_s]^{-1}$ with ν and Y respectively the Poisson coefficients and Young moduli of the tip and sample materials.

Spatial resolution of AFM in vacuum

Resolution limits of STM and AFM are given by the structural properties of the atomic wave functions of the probe tip and the sample.

STM is sensitive to the most loosely bonded electrons with energy at the Fermi level.

AFM responds to all electrons, including core electrons.

Because the electrons at the Fermi level are spatially less confined than core electrons that contribute to AFM images, in theory AFM should be able to achieve even greater spatial resolution than STM.

Experimental advances that made high-resolution AFM frequency modulation AFM (FM-AFM), where the cantilever oscillates at fixed amplitude and the frequency is used as a feedback signal.

Silicon cantilevers with a spring constant of 10 N/m that oscillates with amplitude on the order of 10 nanometers.

Spatial resolution could be increased by the introduction of quartz cantilevers with stiffness on the order of 1 kN/m, allowing the use of sub-nanometers amplitudes.

The direct evaluation of higher harmonics in the cantilever motion has enabled a further increase in spatial resolution.

- Operation

AFM can be viewed as an extension of the toddlers way of ‘grasping’ the world by touching and feeling as

Likewise, one could argue that stylus profilometry is a predecessor of AFM.

However, AFM and stylus profilometry have as much in common as a candle and a laser. Both of the latter generate light, and even though candles are masterpieces of engineering, the laser is a much more advanced technological device requiring a detailed knowledge of modern quantum mechanics.

While stylus profilometry is an extension of human capabilities that have been known for ages and works by classical mechanics.

AFM requires a detailed understanding of the physics of chemical bonding forces and the technological prowess to measure forces that are several orders of magnitude smaller than the forces acting in profilometry.

Established in 1981, is the first instrument that has allowed to image surfaces with atomic resolution in real space. The atomic imaging of the 7×7 reconstruction of Si (111) by STM in 1983 has later helped to solve one of the most intriguing problems of surface science at that time and establish the dimer-adatom-stacking fault model by Takayanagi et al. [Takayanagy, K. et al., J. Vac. Sci. Technol. A **3**, 1502 (1985)]. The capability of atomic resolution by STM provided immediate evidence for the enormous value of this instrument as a tool for surface scientists.

STM can only be used on conductive surfaces. Given that many surfaces of technological interest are conducting or at least semiconducting, this may not seem to be a severe shortcoming. One might think that an STM is capable of mapping the surface of a metallic surface at ambient conditions. However, this is not feasible, because the pervasive layer of oxides and other contaminants occurring at ambient conditions prevents stable tunneling conditions. Electrical conductivity is a necessary, but not a sufficient condition for a surface to be imaged by STM with atomic resolution, because surfaces need to be extremely clean on an atomic level. Except for a few extremely inert surfaces such as graphite, atomic resolution is only possible in an ultra-high vacuum with a pressure on the order of 10^{-8} Pa and special surface preparation.

The invention of the AFM by Binnig and its introduction by Binnig, Quate and Gerber opened the possibility of obtaining true atomic resolution on conductors and insulators.

Also, the forces that acted between tip and sample were often orders of magnitudes larger than the forces that a tip with a single front atom was expected to be able to sustain. Therefore, it was commonly assumed that *many* tip atoms interacted with the surface at the same time in these early experiments.

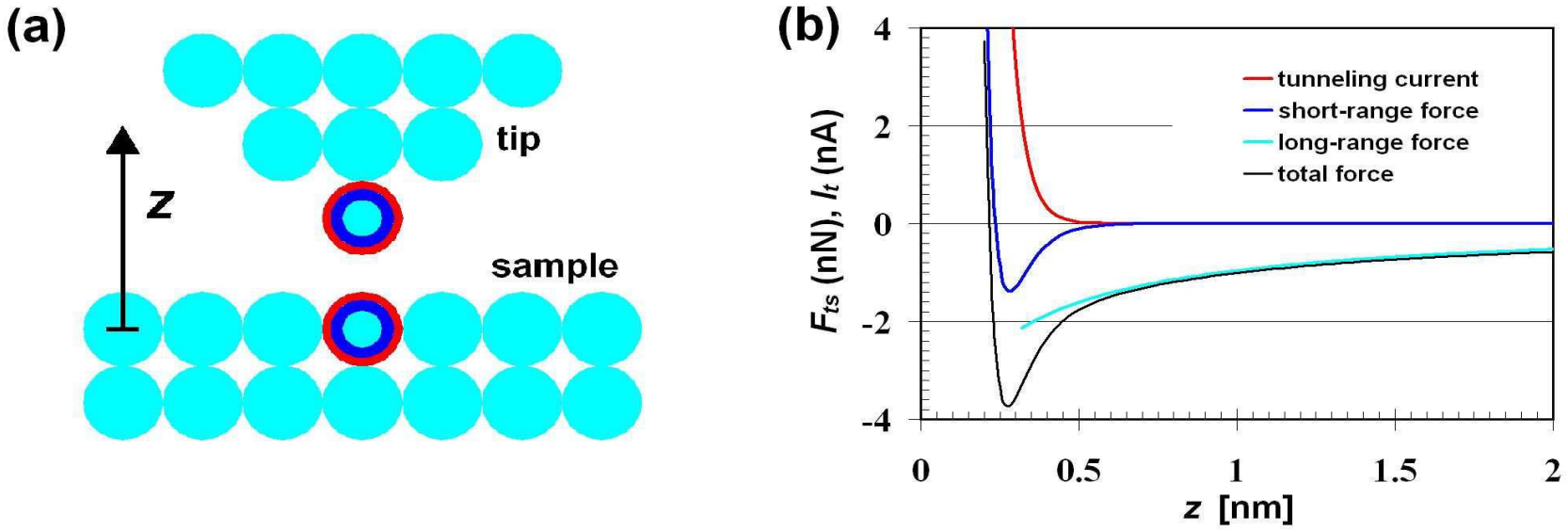

Figure 1: (a) Schematic view of a tip and a sample in a STM or AFM. The diameter of a metal atom is typically 0.3 nm. (b) Qualitative distance dependence of tunneling current, long- and short-range forces. The tunneling current increases monotonic with decreasing distance, while the force reaches a minimum and increases for distances below the bond length.

The difference between *apparent* and *true* atomic resolution of a tip with many atomic contacts can be illustrated by a macroscopic example: When profiling an egg crate with a single egg, its trajectory would represent the overall periodicity of the crate as well as a dented hump or a hole. However, when profiling one egg crate with another egg crate, again its periodicity would be retained, but holes or dented humps would pass undetected. A similar effect can occur when an AFM tip probes a surface.

Figure 1 (a) shows a schematic view of a sharp tip for STM or AFM close to a crystalline sample and Fig. 1 (b) is a plot of the tunneling current and forces between tip and sample. When tip and sample are conductive and a bias voltage is applied between them, a tunneling current can flow. The red curve in Fig. 1 (b) shows the distance dependence of the tunneling current It. The exponential decay of It with distance at a rate of approximately one order of magnitude per 100 pm distance increase is the key physical characteristic that makes atomic resolution STM possible. Because of its strong decay rate, the tunneling current is spatially confined to the front atom of the tip and flows mainly to the sample atom next to it (indicated by red circles in Fig. 1 (a)). A second helpful property of the tunneling current is its monotonic distance dependence. It is easy to build a feedback mechanism that keeps the tip at a constant distance: if the actual tunneling current is larger than the set point, the feedback needs to withdraw the tip and vice versa.

The tip sample force F_{ts}, in contrast, does not share the key characteristics of the tunneling current. First, F_{ts} is composed of long-range background forces depicted in light-blue in Fig. 1(b) and originating from the atoms colored light-blue in Fig. 1 (a) and a short-range component depicted in blue in Fig. 1 (b) and confined to the atoms printed in blue in Fig. 1 (a). Because the short-range force is not monotonic, it is difficult to design a feedback loop that controls distance by utilizing the force. A central task to perfect AFM is therefore the isolation the front atom's force contribution and the creation of a linear feedback signal from it.

- AFM measurements

In addition, high precision scales take about one second to acquire a weight measurement so the bandwidth is only 1 Hz. The force meters in AFM, in contrast, require a force resolution of at least 1 nN at a typical bandwidth of 1 kHz.

Most force meters determine the deflection q` of a spring with given spring constant k that is subject to a force F with F = q`· k. Measuring small spring deflections is subject to thermal drift and other noise factors, resulting in a finite deflection measurement accuracy δq`. The force resolution is thus given by $\delta$F = $\delta$q`· k and soft cantilevers provide less noise in the force measurement.

In contact-mode AFM, where the tip feels small repulsive forces from the sample surface, the cantilever should be softer than the bonds between surface atoms (estimated at ~10 N/m), otherwise the sample deforms more than the cantilever. Because of noise and stability considerations, spring constants below 1 N/m or so have been chosen for AFM in contact mode.

However, atomic forces are usually attractive in the distance regime that is best suited for atomic resolution imaging (approximately a few hundred picometers before making contact), and soft cantilevers suffer from a “jump-to-contact” phenomenon, i.e. when approaching the surface, the cantilever snaps towards the surface ended by an uncontrolled landing.

The long-range attractive forces have been compensated in these experiments by pulling at the cantilever (negative loading force) after jump-to-contact or by immersing cantilever and sample in water to reduce the van der Waals attraction.

In summary, AFM shares the challenges that are already known from STM. Four extra problems for atomic resolution AFM:

- Jump-to-contact
- Non-monotonic short range forces
- Strong long-range background forces
- Instrumental noise in force measurements.

- Frequency modulation AFM

Dynamic AFM modes help to alleviate two of the four major AFM challenges. Jump-to-contact can be prevented by oscillating the cantilever at large enough amplitude A such that the withdrawing force on the cantilever given by $k \times A$ is larger than the maximal attractive force. Because the noise in cantilever deflection measurements has a component that varies in intensity inversely with frequency (1/f-noise), dynamic AFM modes is less subject to noise than quasistatic operating modes. Non-monotonic interactions and strong long-range contributions are still present.

In amplitude modulation AFM, the cantilever is driven at a constant frequency and the vibration amplitude is a measure of the tip-sample interaction. In 1991, Albrecht et al. [Albrecht, T.R. et al., J. Appl. Phys. **69**, 668 (1991)] have shown that frequency modulation (FM) AFM offers even less noise at larger bandwidth than amplitude modulation AFM. In FM-AFM, a cantilever with a high quality factor Q is driven to oscillate at its eigenfrequency by positive feedback with an electronic circuit that keeps the amplitude A constant.

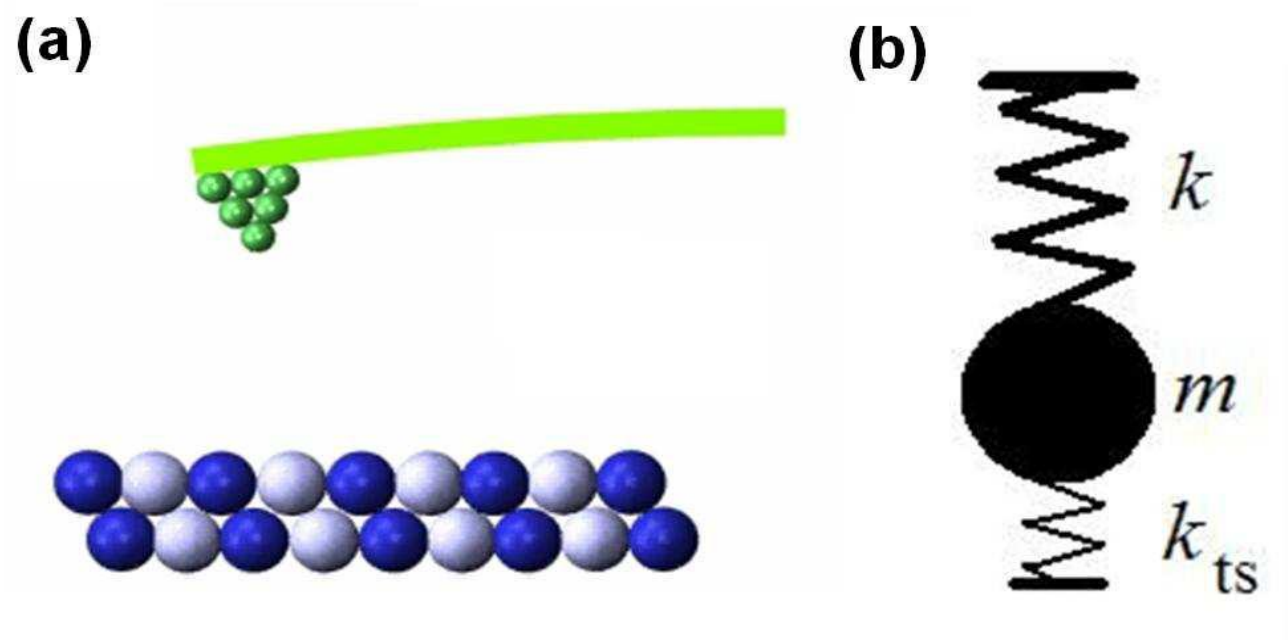

Figure 2: (a) Schematic view of a vibrating tip close to a sample in a dynamic AFM. The forces that act between the tip and the sample F_{ts} cause a detectable change in the oscillation properties of the cantilever. (b) Mechanical equivalent of (a). The free cantilever with stiffness k and effective mass m can be treated as a harmonic oscillator with an eigenfrequency $f_0 = (k/m)^{1/2}/(2\pi)$. The bond between tip and sample with its stiffness k_{ts} alters the resonance frequency to $f = ([k + k_{ts}]/m)^{1/2}/(2\pi)$. When the oscillation amplitude of the cantilever is large, kts can vary significantly within one oscillation cycle, requiring averaging.

A cantilever with a stiffness of k and effective mass m has an eigenfrequency given by $f_0 = 1/(2\pi)\ (k/m)^{1/2}$. When the cantilever is exposed to a tip-sample force gradient k_{ts}, its frequency changes instantly to $f = f_0 + \Delta f = 1/(2\pi)(k`/m)^{1/2}$ where $k` = k + k_{ts}$ (see Fig. 2). When k_{ts} is small compared to k, the square root can be expanded and the frequency shift is simply given by:

$$\Delta f(z) = \frac{f_0}{2k} k_{ts}(z)$$

This formula is only correct if k_{ts} is constant over the distance range from z − A to z + A that is covered by the oscillating cantilever.

Imagine an atom magnified to a size of an orange with a diameter of 8 cm. The range of the bonding force is then only 4 cm or so and the front atom of the cantilever would approach from a distance of 20m and only in the last few centimeters of its oscillation cycle would feel the attractive bonding forces from the sample atom next to it. On the other hand, force gradients can be quite large in chemical bonds. According to the well-known Stillinger-Weber potential, a classic model potential the interaction of Si atoms in the solid and liquid phases, a single bond between two Si atoms has a force gradient of k_{ts} = +170 N/m at the equilibrium distance of z = 235 pm and k_{ts} = −120 N/m when the two Si atoms are at a distance of z = 335 pm. Because of the relatively large values of interatomic force gradients, even cantilevers with stiffness on the order of 1 kN/m should be subject to significant frequency shifts when oscillating at small amplitudes. Nevertheless, the large-amplitude FM technique has celebrated great successes by imaging metals, semiconductors and insulators with true atomic resolution.